Alterations of tibialis anterior muscle activation pattern in subjects with type 2 diabetes and diabetic peripheral neuropathy

Favretto, M A; Cossul, S; Andreis, F. R.; Nakamura, L R.; Ronsoni, M F; Tesfaye, S.; Selvarajah, D; Marques, J L B

Alterations of tibialis anterior muscle activation pattern in subjects with type 2 diabetes and diabetic peripheral neuropathy

Abstract

Diabetic peripheral neuropathy (DPN) is associated with loss of motor units (MUs), which can cause changes in the activation pattern of muscle fibres. This study investigated the pattern of muscle activation using high-density surface electromyography (HD-sEMG) signals from subjects with type 2 diabetes mellitus (T2DM) and DPN. Thirty-five adults participated in the study: 12 healthy subjects (HV), 12 patients with T2DM without DPN (No-DPN) and 11 patients with T2DM with DPN (DPN). HD-sEMG signals were recorded in the tibialis anterior muscle during an isometric contraction of ankle dorsiflexion at 50% of the maximum voluntary isometric contraction (MVIC) during 30-s. The calculated HD-sEMG signals parameters were the normalised root mean square (RMS), normalised median frequency (MDF), coefficient of variation (CoV) and modified entropy (ME). The RMS increased significantly $(p = 0.001)$ with time only for the DPN group, while the MDF decreased significantly $(p < 0.01)$ with time for the three groups. Moreover, the ME was significantly lower $(p = 0.005)$, and CoV was significantly higher $(p = 0.003)$ for the DPN group than compared to the HV group. Using HD-sEMG, we have demonstrated a reduction in the number of MU recruited by individuals with DPN. This study provides proof of concept for the clinical utility of this technique for identifying neuromuscular impairment caused by DPN.

Keywords: Diabetic neuropathies; High-density surface electromyography; Motor unit recruitment; Tibialis anterior muscle.

1. Introduction

Diabetic peripheral neuropathy (DPN) is a common complication of diabetes mellitus resulting in significant morbidity and mortality [1–4]. Symptomatic motor dysfunction occurs only in more advanced stages of DPN and consists of muscle wasting, gait changes and distal weakness of the lower limbs [5–8]. Besides motor dysfunctions, subjects with diabetes and DPN also present a change in the proportion of fibre type, favouring the presence of type II fibres over type I fibres muscle [9], which explains why dysfunctions occur initially in muscles with a higher proportion of type I fibres, such as the tibialis anterior (TA) [9,10]. Additionally, the change in the proportion of muscle fibres may explain premature muscle fatigue and low tolerance to exercises such as walking, cycling, and ankle extension in individuals with diabetes [11,12].

Studies using intramuscular electromyography (iEMG) have demonstrated chronic reinnervation in the TA muscle in early, subclinical DPN. This evidence includes the reduction of the muscle fibre conduction velocity, increase of the instability in the single muscular fibre potential, increase in the density of the muscular fibre and reduction in the number and the rate of firing of the motor unit (MU) [13–17]. Hence, quantifying motor dysfunction with iEMG could serve as an early biomarker for DPN and may identify individuals for early targeted physical therapy intervention to attenuate further worsening of the disease [13–17]. Nevertheless, iEMG is an invasive, painful and costly method with poor reproducibility [18], providing limited information about activity at the whole-muscle level [19].

As a solution to this problem, studies have evaluated non-invasive MU recruitment strategies using high-density surface electromyography (HD-sEMG) techniques [20–22], since HD-sEMG enables the acquisition of a topographical

representation of the spatial distribution pattern of muscle activation [23]. Previous studies have shown that the spatial distribution of muscle activation during isometric contractions is heterogeneous [21], which may be explained by the recruitment of different types of muscle fibres [20]. Moreover, studies have used the spatial distribution pattern of muscle activation to estimate MU recruitment patterns [24–28]. Thus, by evaluating the homogeneity of the spatial distribution pattern of muscle activation, it would be possible to assess alterations in the recruitment of the muscular fibres in individuals with diabetes and DPN.

Therefore, this work aims to evaluate the homogeneity of TA muscle activation patterns in healthy individuals compared to individuals with diabetes with and without DPN, given that the TA muscle is associated with the MU loss in the initial stages of DPN [13–17]. We hypothesised that due to the compensatory process characterised by the continuous loss of the MU coupled with compensatory reinnervation, the individuals with diabetes and DPN would present alterations in the MU recruitment pattern, which will be reflected in alterations in the spatial distribution pattern of muscle activation.

2. Materials and Methods

2.1. Subjects

Twenty-three individuals with type 2 diabetes (T2DM) were recruited from the University Hospital of the Federal University of Santa Catarina, at the Endocrinology and Metabology Unit, and twelve healthy volunteers (HV) were recruited elsewhere [3,29]. Anthropometric and clinical data (DM duration, HbA1c test result, use of medications and presence of complications) were obtained previously. Individuals with diabetes were divided into T2DM without DPN (No-DPN, n=12) and patients with T2DM with DPN (DPN, n=11) using the Toronto Consensus minimum criteria definition for DPN [3,29]. The neuropathic symptoms were assessed using the Neuropathy Total Symptom Score – 6 (NTSS-6) questionnaire [30]. A trained clinician performed a standardised physical examination and evaluated tactile sensitivity with a 10 g Semmes-Weinstein monofilament, vibratory perception with a 128 Hz tuning fork and ankle reflexes [3,29]. Inclusion criteria were age over 18 but less than 65 years old and T2DM diagnosis based on the World Health Organization definition [31]. Exclusion criteria were minor/major limb amputation or other physical, neurological, musculoskeletal deficiencies, *e.g.* stroke, cerebral palsy, polio, arthritis; sight limiting diabetic retinopathy, severe nephropathy, chronic kidney disease stage 4-5, lower limb oedema; active diabetic foot ulceration [10]. All study procedures followed the principles of the Declaration of Helsinki.

Table 1. Demographic and clinical data of the participants.

	HV	No-DPN	DPN
n	12	12	11
Age (years)	49.8 (5.1) *	60.0 (5.7) *	55.7 (7.0)
Height (cm)	166 (8.0)	163 (9.0)	167 (8.0)
Weight (kg)	78.7 (12.6)	83.1(13.2)	84.3 (11.2)
BMI	28.16 (3.05)	31.50 (5.97)	30.01 (2.47)
MVIC (N)	286.46 (66.8) *†	228.52 (44.5) *	212.68 (73.6) †
HbA1c (%)	ND	7.3 (1.4)	8.05 (2.7)
HbA1c (mmol/mol)	ND	56 (15)	76 (29)
Sex (male/female)	6/6	6/6	5/6
Diabetes mellitus duration (years)	ND	8.0 (6.0)	10.0 (5.0)
Subcutaneous tissue thickness (mm)	6.08 (2.5)	7.66 (4.6)	6.72 (2.0)

Note: Values are presented as mean ± SD. *Abbreviations:* HV, healthy volunteers; NO-DPN, Individuals with type 2 diabetes without diabetic peripheral neuropathy; DPN, Individuals with type 2 diabetes with diabetic peripheral neuropathy; BMI, body mass index; MVIC, maximum voluntary isometric contractions; HbA1c, glycated haemoglobin; ND, not done. $p < 0.05$ when comparing HV to No-DPN. † $p < 0.05$ when comparing HV to DPN.

2.2. Experimental Protocol

Participants stayed seated with hip and knee flexed at a 90º angle and the ankle in a neutral position at a 90º angle to the leg. The foot of the dominant leg was fixed on a custom-made dynamometer (Figure 1). The dynamometer measured the force using a strain-gauge load cell (traction/compression, 60-kg range), digitised with a 24-bit A/D converter and a sampling frequency of 80 Hz. The reliability of this dynamometer has been described elsewhere [32]. The participants performed three maximum voluntary isometric contractions (MVIC) of the ankle dorsiflexion with a 5-s duration. A 2-minute rest interval separated these tests. To ensure that MVIC was achieved during the trials, participants were verbally stimulated to produce the maximum effort. The highest value of the three MVICs was used as a reference for the submaximal level definition. After fixation of the HD-sEMG matrix of electrodes in the TA muscle, the subjects performed a submaximal voluntary isometric contraction of ankle dorsiflexion in 50% of the MVIC value. The contraction was maintained for 30-s. Real-time visual feedback of the force developed was provided to the participants on a computer screen (Figure 1). Throughout the experimental procedure, the room was maintained at a temperature of approximately 23 °C.

Figure 1. Illustration of the experimental protocol to record the HD-sEMG signals.

ELSCH064NM4

Ground electrode   Isolated dual power supply
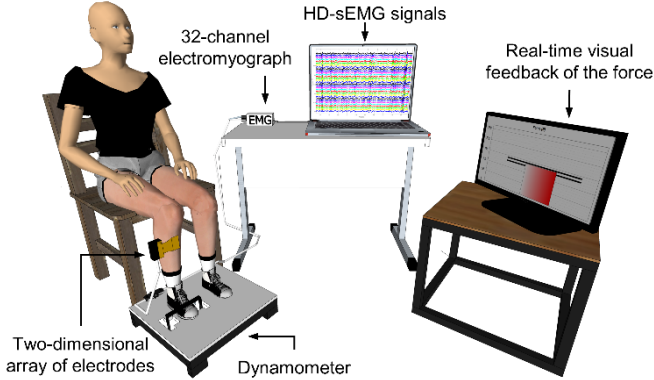
2.3. Data Acquisition

The HD-sEMG signals were recorded from the TA muscle using a 32-channel electromyography system, unity gain and digitised with a 24-bit A/D converter at 2 kHz per channel [33]. We used a two-dimensional array of 64 electrodes (ELSCH064NM4, OT Bioelettronica, Torino, Italy) for the acquisition, consisting of thirteen rows and five columns, with a 1 mm diameter and a distance between electrodes of 4 mm. The signals were detected in a simple longitudinal differential configuration, using nine rows and four columns of the array, *i.e.* 36 electrodes with a bipolar configuration set up in the hardware, resulting in 32 single differential EMG signals (Figure 2). Before attaching the matrix, the skin was cleaned with alcohol and gauze. Then, the electrode matrix was fixed using fixation adhesive and positioned according to guidelines from the Surface EMG for Non-invasive Assessment of Muscles (SENIAM) and the Atlas of Muscle Innervation Zones [34]. The cavities on the electrodes, formed due to the adhesive, were filled with conductive paste (CC1, OT Bioelettronica, Turin, Italy). A reference electrode was also fixed on the tuberosity of the tibia.

Figure 2. Sampling in a differential configuration column-wise. There are four columns (C) and nine rows (R) resulting in 32 signals $[C \times (R-1)]$.
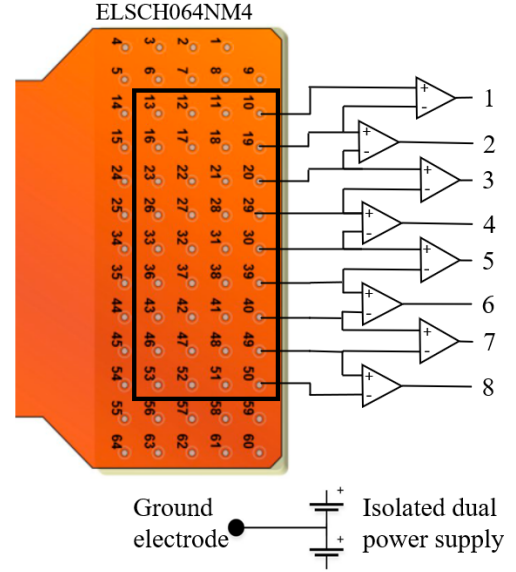
2.4. Signal Processing

The participants followed a step pattern of force. The signals from the first 2.0 seconds, in which participants used to reach the force level, and the last 3.0 seconds that participants released the contraction were excluded from the analysis, resulting in a signal with a 25-s duration. The acquired signals were digitally filtered in the MATLAB R2018 software (MathWorks, MA, USA) by an eighth order Butterworth bandpass filter from 10 to 400 Hz. A second-order 60 Hz notch filter and its subsequent five harmonics were applied to the signals to reduce power line interference. Noisy signals were visually inspected and reconstructed based on the interpolation of the signals from the two neighbouring channels [35].

The following variables were extracted from the 32 bipolar signals: root means square (RMS) and median frequency (MDF) [36]. The 32 RMS and MDF values were normalised by the mean value of the first second of contraction. To quantify the heterogeneity of spatial distribution of muscle activation (represented as topographical maps), we used the coefficient of variation (CoV) and the modified entropy (ME), which were the primary study outcome measures. The CoV was defined as the standard deviation of the 32 absolute RMS values, divided by the mean of the 32 absolute RMS values obtained in each topographic map [27]. The ME was calculated for 32 absolute RMS values according to the method published by Farina et al. (2008). It indicates the degree of homogeneity of muscle activation, with higher values corresponding to a more uniform distribution of the RMS values over the electrode matrix [20]. It is important to notice that a decrease in the ME and an increase in CoV, respectively, represents an

increase in the heterogeneity of the spatial distribution of the electrical potentials recorded by the electrode matrix [27].

Muscle activation level was assessed using the 32 absolute RMS values (*i.e.* referent to each channel) and categorised into three levels of activation by the peak percentage of RMS value, low (RMS peak < 33%), middle (33.3% ≥ RMS peak < 66.6%) and high (RMS peak ≥ 66.6%), following the methodology published by Watanabe et al. (2012b) [37]. All variables (normalised RMS, normalised MDF, CoV, ME and level of muscle activation) were calculated over time using 0.5-s rectangular windows without overlap. Mean values were obtained for 0 − 5s, 5.5 − 10s, 10.5 − 15s, 15.5 − 20s and 20.5 − 25s of the contraction time.

The graphical representation of the spatial distribution for the absolute RMS value of the signal of the HD-sEMG was shown as a colour map (*i.e.* topographical map). For a sharper picture, the absolute RMS colour maps were interpolated by a factor of 8. However, only the 32 original values (referent to each channel) were used for calculating all the variables (normalised RMS, normalised MDF, CoV, ME, level of muscle activation).

2.5. Statistical Analysis

Statistical analyses were performed using R (R Core Team, 2018) [38]. All data are provided as the mean and standard deviation. The normality distribution of the data was tested with the Shapiro-Wilk test. Subgroup comparisons of normally distributed data were performed using a one-way ANOVA followed by a Tukey post hoc test. For non-normal data, we performed a Kruskal–Wallis test followed by Dunn-Bonferroni post hoc. Statistical differences in normalised RMS, normalised MDF, ME, CoV and number of channels representing the muscle activation level were analysed using two-way analysis of variance (ANOVA) with repeated measures. The within-subjects factor was the time; the between-subjects factor was the group (*i.e.*, HV, No-DPN, DPN). Tukey pairwise comparisons followed significance revealed by ANOVA. Residuals were analysed graphically to assess the normality assumption. The significance level adopted was 0.05.

3. Results

There was no significant difference between the groups when analysing gender distribution, height, weight, BMI, and subcutaneous tissue thickness (Table 1). There were also no statistically significant differences in the duration of diabetes and glycated haemoglobin (HbA1c) between the diabetes subgroups. Subjects with No-DPN were, however, older compared to HV (*p* = 0.01).

Figure 3 shows a representation of the RMS spatial distribution of the HD-sEMG as a colour map (*i.e.*

topographical map), at selected intervals, during submaximal isometric ankle dorsiflexion of an individual from each study group. In the DPN subjects, there is a large area with low RMS values. This is also shown in the graph with the number of channels categorised into low, middle, and high muscle activation levels in Figure 4. At low activation levels, the post hoc analysis revealed that the number of channels was significantly higher for the DPN group compared to the HV group (*p* = 0.03). At middle activation levels, the post hoc analysis revealed that the number of channels was significantly lower for the DPN group compared to the HV group (*p* = 0.02). At high activation levels, there was no significant difference between the groups. In addition, there was no significant difference in time for any groups at low, middle, and high activation levels. Hence, the three activation levels for each channel were illustrated only at the 0-5s time point in Figure 4.

Figure 3. Illustration of the spatial distribution of root mean square (RMS) values of high-density surface electromyography (HD-sEMG) shown as a colour map at selected periods during sustained contraction of a healthy individual (HV), an individual with type 2 diabetes (T2DM) without diabetic peripheral neuropathy (No-DPN) and an individual with T2DM with diabetic peripheral neuropathy (DPN).
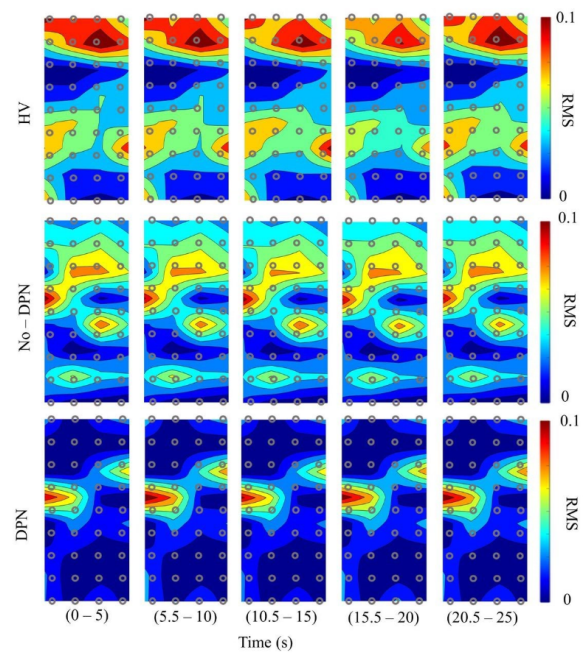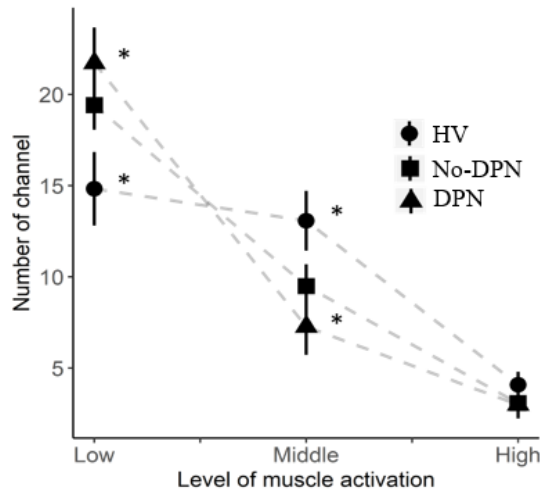

Figure 4. The number of channels for three root mean square (RMS) levels of high-density surface electromyography (HD-sEMG) signal amplitude, at 0–5s. * *p* < 0.05 significant difference between the groups.

For the ME, there was a significant effect of time (*p* = 0.02) and group (*p* = 0.006) and no significant group-by-time interaction (*p* = 0.99) (Figure 5(a)). The post hoc analysis revealed that the ME in the DPN group was significantly (*p* = 0.005) lower than in the HV group. As for the effect of time, there was a decrease in the ME value in the fourth period (*p* = 0.02). For the CoV, there was a significant effect of group (*p* = 0.003) and time (*p* = 0.03). The post hoc analysis revealed that the CoV in the DPN group was significantly higher than in the HV group (*p* = 0.002) (Figure 5(b)). As for the effect of time, there was an increase in the CoV value in the fourth period. There were no significant differences between the No-DPN and the DPN groups for the variables ME (*p* = 0.072) and CoV (*p* = 0.086).

For the normalised RMS, there was a significant group-by-time interaction (*p* = 0.001), resulting in an increase of the RMS magnitude with time in the DPN group (Figure 5(c)). For the other two groups (HV and No-DPN), the effect of time was not significant. For the normalised MDF values, there was a significant decrease in the magnitude with time for the three groups (*p* < 0.01) and no significant difference between the groups (Figure 5(d)).

Figure 5. Graphics of the parameters analysed of high-density surface electromyography (HD-sEMG) signals, at selected periods, during sustained contraction of the groups: healthy volunteers (HV), individual with type 2 diabetes (T2DM) without diabetic peripheral neuropathy group (No-DPN) and individual with T2DM with diabetic peripheral neuropathy (DPN). (a) Modified entropy (ME). (b) Coefficient of variation (CoV). (c) Normalised root means square (RMS). (d) Normalised median frequency (MDF). + p < 0.01 group-by-time significant interaction. # p < 0.01 significant difference in time compared with 0–5-s period. * p < 0.05 significant difference between the groups.
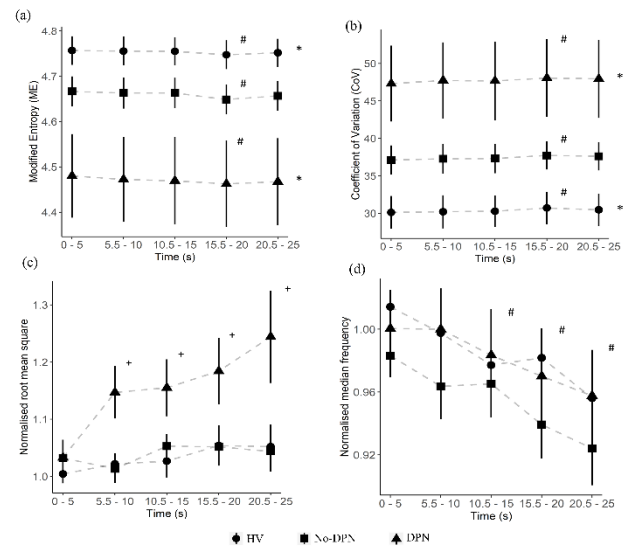
For the MVIC, there was a significant effect on the group (*p* = 0,018). The post hoc analysis revealed that the groups No-DPN and DPN had significantly lower force compared to HV (*p* = 0.04 and *p* = 0.02, respectively) (Figure 6).

Figure 6. Maximum voluntary isometric contractions of the groups' healthy volunteers (HV), subjects with type 2 diabetes (T2DM) without diabetic peripheral neuropathy (No-DPN) and individuals with T2DM with diabetic peripheral neuropathy (DPN). * *p* < 0.05 significant difference between the groups.
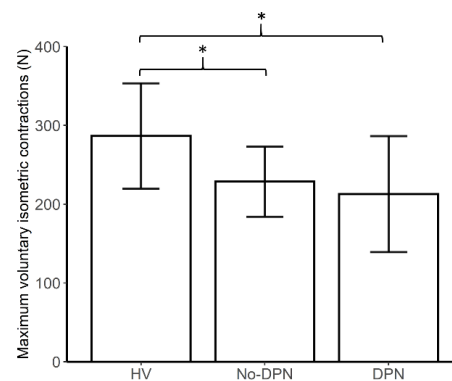
4. Discussion

This study aimed to evaluate the spatial distribution of the HD-sEMG signals in the TA muscle in healthy volunteers compared with diabetic individuals with and without DPN. To the best of our knowledge, this is the first study to evaluate alterations in the topographic maps of the TA muscle of individuals with DPN. Watanabe et al. [37] have previously evaluated changes in the topographical maps in subjects with T2DM in the vastus lateralis muscle. Nevertheless, the degree of DPN was not assessed. In addition, it is essential to emphasize that the vastus lateralis muscle has a greater proportion of type II fibres, which are

5

more resistant to changes caused by DPN [10]. On the other hand, the TA muscle has a higher proportion of type I muscle fibres, which are more sensitive to changes caused by diabetes and DPN [9].

The main results were: (1) higher CoV and lowered ME in DPN subjects, (2) increase in the normalised RMS value with time in subjects with DPN and decreased normalised mean MDF over time in all groups and (3) lower MVIC force in patients with diabetes compared to HV (Table 1). These results confirm the hypothesis that there is increased heterogeneity in the spatial distribution pattern of muscle activation in individuals with diabetes with and without DPN. Watanabe et al. 2012b also found changes in the homogeneity of the spatial distribution of topographic maps in the vastus lateralis muscle in T2DM individuals but did not account for the presence of DPN [37].

The heterogeneity in the spatial distribution of HD-sEMG potentials observed in DPN subjects can be explained by a greater number of electrodes with low (RMS peak < 33%) than high RMS values (RMS peak $\geq$ 66.6%). In contrast, considering the HV group, the RMS values were closer to the mean value (33.3% $\geq$ RMS peak < 66.6%). The heterogeneity in the spatial distribution of HD-sEMG potentials can be explained by spatial inhomogeneity in the location of different types of muscle fibres and a clustering of muscle fibre innervated by one MU in a limited territory [21]. Therefore, as the spatial distribution may reflect the recruitment of MU, we could assume that patients with DPN are recruiting a limited number of MUs. These findings agree with Allen et al. (2013a), who found that subjects with DPN recruited fewer MUs during submaximal isometric contractions [13].

The heterogeneity of the HD-sEMG potential distribution can also result from early muscle fatigue [20,21]. Although all participants maintained the level of force during 30-s, subjects with DPN demonstrated early indications of myoelectric manifestation of muscle fatigue (*i.e.*, a significant increase in RMS and decreased MDF over time) [39,40]. Allen et al. (2015) also showed that individuals with DPN have premature muscular fatigue during isometric contractions of ankle dorsiflexion [41]. Furthermore, Oberbach et al. 2006 showed that patients with T2DM have a relatively higher proportion of fast-twitch muscle fibres (type II) and a decrease in slow-twitch muscle fibres (type I, responsible for muscle endurance) [9]. Thus, a combination of altered muscle fibre composition and MU loss may explain premature muscular fatigue in DPN subjects. Further research is needed to establish the relative contribution of muscle fatigue and MU loss on the changes in the spatial distribution pattern of muscle activation.

We also found that subjects with diabetes (with and without DPN) had significantly lower MVIC force than HV

subjects. This agrees with previous studies that have also reported that muscle weakness affects patients in the early stages of the disease [42]. Longer duration of diabetes and chronic complications such as DPN resulted in more significant loss of muscle force due to loss of MUs. The reduction in the ankle dorsiflexion force is also associated with plantar ulcers in DPN [43–46] and an increased risk of falls [47–50].

Although there are significant differences in the force and spatial distribution pattern of the topographic maps between DPN and HV, there was no significant difference between No-DPN and DPN subgroups. However, post hoc analysis indicated suggestive evidence of a difference between No-DPN and DPN groups since p values were close to 0.05 for the ME (p = 0.072) and the CoV (p = 0.086). Furthermore, since this study had a significant effect size (0.4), the sample size estimate demonstrates that with an increase of approximately five individuals in each group, these parameters will probably also present statistical differences for No-DPN and DPN.

The age difference between the groups could have influenced these assessments; however, no significant statistical differences were found within the groups when considering age as a covariate. Thus, a more extensive study with a matched sample of subjects is needed to confirm the findings of this study.

5. Conclusions

This study showed that individuals with DPN recruit a limited number of MUs, resulting in a reduction in the isometric force of ankle dorsiflexion and myoelectric manifestations of muscle fatigue. Also, we demonstrated that the evaluation of changes in the spatial distribution of HD-sEMG signals is a promising technique for identifying neuromuscular alterations caused by DPN. These results point to further research investigating the relationship between abnormalities in HD-sEMG signals and clinical assessments of DPN patients. Future studies could also evaluate whether early targeted physical therapy intervention guided by HD-sEMG could improve clinical outcomes.

References

[1] Pop-Busui R, Boulton AJM, Feldman EL, Bril V, Freeman R, Malik RA, et al. Diabetic neuropathy: A position statement by the American diabetes association. Diabetes Care. 2017;40:136–54.

[2] Selvarajah D, Kar D, Khunti K, Davies MJ, Scott AR, Walker J, et al. Diabetic peripheral neuropathy: advances in diagnosis and strategies for screening and early intervention. LANCET

Diabetes Endocrinol. Elsevier Ltd; 2019;8587. Available from: http://dx.doi.org/10.1016/S2213-8587(19)30081-6

[3]   Tesfaye S, Boulton AJM, Dyck PJ, Freeman R, Horowitz M, Kempler P, et al. Diabetic neuropathies: Update on definitions, diagnostic criteria, estimation of severity, and treatments. Diabetes Care. American Diabetes Association; 2010 [cited 2017 Mar 20];33:2285–93. Available from: http://www.ncbi.nlm.nih.gov/pubmed/20876709

[4]   International Diabetes Federation. IDF Diabetes Atlas - 2019. 9 th. IDF Diabetes Atlas, 9th Ed. Brussels: International Diabetes Federation; 2019.

[5]   Andreassen CS, Jakobsen J, Andersen H. Muscle Weakness: A Progressive Late Complication in Diabetic Distal Symmetric Polyneuropathy. Diabetes. 2006;55:806–12. Available from: http://diabetes.diabetesjournals.org/cgi/doi/10.2337/diabetes.55.03.06.db05-1237

[6]   Andersen H. Motor dysfunction in diabetes. Diabetes Metab. 2012;28:89–92.

[7]   Andersen H, Jakobsen J. A Comparative Study of Isokinetic Dynamometry and Manual Muscle Testing of Ankle Dorsal and Plantar Flexors and Knee Extensors and Flexors. Eur Neurol. 1997;37:239–42. Available from: https://www.karger.com/Article/FullText/117450

[8]   Andersen H, Gadeberg PC, Brock B, Jakobsen J. Muscular atrophy in diabetic neuropathy: a stereological magnetic resonance imaging study. Diabetologia. 1997;40:1062–9. Available from: http://link.springer.com/10.1007/s001250050788

[9]   Oberbach A, Bossenz Y, Lehmann S, Niebauer J, Adams V, Paschke R, et al. Altered Fiber Distribution and Fiber-Specific Glycolytic and Oxidative Enzyme Activity in Skeletal Muscle of Patients With Type 2 Diabetes. Diabetes Care. 2006;29:895–900.

[10]   Butugan MK, Sartor CD, Watari R, Cecília M, Martins S, Ortega NRS, et al. Multichannel EMG-based estimation of fiber conduction velocity during isometric contraction of patients with different stages of diabetic neuropathy. J Electromyogr Kinesiol. Elsevier Ltd; 2014;24:465–72. Available from: http://dx.doi.org/10.1016/j.jelekin.2014.04.007

[11]   Larsen S, Ara I, Rabøl R, Andersen JL, Boushel R, Dela F, et al. Are substrate use during exercise and mitochondrial respiratory capacity decreased in arm and leg muscle in type 2 diabetes? Diabetologia. 2009;52:1400–8.

[12]   Regensteiner JG, Bauer T a, Reusch JE, Brandenburg SL, Sippel JM, Vogelsong a M, et al. Abnormal oxygen uptake kinetic responses in women with type II diabetes mellitus. J Appl Physiol. 1998;310–7. Available from: http://jap.physiology.org/content/85/1/310.short

[13]   Allen MD, Choi IH, Kimpinski K, Doherty TJ, Rice CL. Motor unit loss and weakness in association with diabetic neuropathy in humans. Muscle Nerve. 2013;48:298–300. Available from: http://doi.wiley.com/10.1002/mus.23792

[14]   Allen MD, Kimpinski K, Doherty TJ, Rice CL. Length dependent loss of motor axons and altered motor unit properties in human diabetic polyneuropathy. Clin Neurophysiol. International Federation of Clinical Neurophysiology; 2013;125:836–43. Available from: http://dx.doi.org/10.1016/j.clinph.2013.09.037

[15]   Bril V, Werb MR, Greene DA, Sima AAF. Single-fiber electromyography in diabetic peripheral polyneuropathy. Muscle Nerve. 1996;19:2–9. Available from: http://doi.wiley.com/10.1002/%28SICI%291097-4598%281996601%2919%3A1%3C2%3A%3AAID-MUS1%3E3.0.CO%3B2-J

[16]   Meijer JWG, Lange F, Links TP, Hoeven JH Van Der. Muscle fiber conduction abnormalities in early diabetic polyneuropathy. Clin Neurophysiol. 2008;119:1379–84.

[17]   Shields RW. Single-fiber electromyography is a sensitive indicator of axonal degeneration in diabetes. Neurology. 1987;37:1394–1394. Available from: http://www.neurology.org/cgi/doi/10.1212/WNL.37.8.1394

[18]   Zwarts MJ, Stegeman DF. Multichannel surface EMG: Basic aspects and clinical utility. Muscle Nerve. Wiley Subscription Services, Inc., A Wiley Company; 2003 [cited 2018 Jan 31];28:1–17. Available from: http://doi.wiley.com/10.1002/mus.10358

[19]   Enoka RM. Physiological validation of the decomposition of surface EMG signals. J Electromyogr Kinesiol. Elsevier; 2019;46:70–83. Available from: https://doi.org/10.1016/j.jelekin.2019.03.010

[20]   Farina D, Leclerc F, Arendt-Nielsen L, Buttelli O, Madeleine P. The change in spatial distribution of upper trapezius muscle activity is correlated to contraction duration. J Electromyogr Kinesiol. 2008;18:16–25.

[21]   Holtermann A, Roeleveld K, Karlsson JS. Inhomogeneities in muscle activation reveal motor unit recruitment. J Electromyogr Kinesiol. 2005;15:131–7.

[22]   Merletti R, Holobar A, Farina D. Analysis of motor units with high-density surface electromyography. J Electromyogr Kinesiol. 2008;18:879–90.

[23]   Merletti R, Farina D. Surface Electromyography: Physiology, Engineering and Applications. Hoboken: Wiley-IEEE Press; 2016.

[24]   Holtermann A, Grönlund C, Stefan Karlsson J, Roeleveld K. Spatial distribution of active muscle fibre characteristics in the upper trapezius muscle and its dependency on contraction level and duration. J Electromyogr Kinesiol. 2008;18:372–81.

[25]   Nishikawa Y, Watanabe K, Takahashi T, Orita N, Kimura H, Matsumoto M, et al. Spatial electromyography distribution pattern of the vastus lateralis muscle during ramp up contractions in Parkinson's disease patients. J Electromyogr Kinesiol. Elsevier; 2017;37:125–31. Available from: http://dx.doi.org/10.1016/j.jelekin.2017.10.003

[26]   Watanabe K, Kouzaki M, Moritani T. Spatial EMG potential distribution of biceps brachii muscle during resistance training and detraining. Eur J Appl Physiol. Springer Berlin Heidelberg; 2015;115:2661–70.

[27] Watanabe K, Kouzaki M, Merletti R, Fujibayashi M, Moritani T. Spatial EMG potential distribution pattern of vastus lateralis muscle during isometric knee extension in young and elderly men. J Electromyogr Kinesiol .Elsevier Ltd; 2012;22:74–9. Available from: http://dx.doi.org/10.1016/j.jelekin.2011.09.010

[28] Nishikawa Y, Watanabe K, Takahashi T, Kimura H, Maruyama H. The effect of medication on vastus lateralis muscle activation patterns in Parkinson's disease patients. J Electromyogr Kinesiol .Elsevier; 2018;42:66–73. Available from: https://doi.org/10.1016/j.jelekin.2018.06.014

[29] Dyck P, Albers JW, Andersen H, Arezzo JC, Biessels G-J, Bril V, et al. Diabetic polyneuropathies: update on research definition, diagnostic criteria and estimation of severity Peter. Diabetes Metab Res Rev. 2011;26:620–8.

[30] Bastyr EJ, Price KL, Bril V. Development and validity testing of the neuropathy total symptom score-6: Questionnaire for the study of sensory symptoms of diabetic peripheral neuropathy. Clin Ther. 2005;

[31] World Health Organization. Global Report on Diabetes. World Heal Organ .2016;978:88. Available from: http://www.who.int/about/licensing/%5Cnhttp://apps.who.int/iris/bitstream/10665/204871/1/9789241565257_eng.pdf

[32] Andreis FR, Favretto MA, Cossul S, Barbetta PA, Marques JLB. Reliability of Maximal Voluntary Isometric Contraction of Ankle Dorsiflexion in Male Subjects. IFMBE Proc. 2019;333–49.

[33] Favretto MA, Cossul S, Andreis FR, Balotin AF, Marques JLB. High Density Surface EMG System Based on ADS1298-front end. IEEE Lat Am Trans .2018;16:1616–22. Available from: https://ieeexplore.ieee.org/document/8444157/

[34] Barbero M, Merletti, R, Rainoldi A. Atlas of Muscle Innervation Zones. 2012;1–146.

[35] Merletti R, Aventaggiato M, Botter A, Holobar A, Marateb H, Vieira TMM. Advances in Surface EMG: Recent Progress in Detection and Processing Techniques. Crit Rev Biomed Eng .Begel House Inc.; 2010 [cited 2017 Feb 16];38:305–45. Available from: http://www.dl.begellhouse.com/journals/4b27cbfc562e21b8,606681d65e2ccb94,45714f720ecf76f5.html

[36] Farina D, Merletti R. Comparison of algorithms for estimation of EMG variables during voluntary isometric contractions. J Electromyogr Kinesiol. 2000;10:337–49.

[37] Watanabe K, Miyamoto T, Tanaka Y. Type 2 diabetes mellitus patients manifest characteristic spatial EMG potential distribution pattern during sustained isometric contraction. Diabetes Res Clin Pract .Elsevier Ireland Ltd; 2012;97:468–73. Available from: http://dx.doi.org/10.1016/j.diabres.2012.03.004

[38] R Code Team. A Language and Environment for Statistical Computing .Vienna, Austria: R Foundation for Statistical Computing; 2018. Available from: https://www.r-project.org/

[39] Merletti R, Knaflitz M, De Luca CJ. Myoelectric manifestations of fatigue in voluntary and electrically elicited contractions. J Appl Physiol .1990;69:1810–20. Available from: http://www.physiology.org/doi/10.1152/jappl.1990.69.5.1810

[40] Farina D, Merletti R, Enoka RM. The extraction of neural strategies from the surface EMG. J Appl Physiol .2004;96:1486–95. Available from: http://jap.physiology.org/content/96/4/1486.abstract

[41] Allen MD, Kimpinski K, Doherty TJ, Rice CL. Decreased muscle endurance associated with diabetic neuropathy may be attributed partially to neuromuscular transmission failure. J Appl Physiol .American Physiological Society Bethesda, MD; 2015 [cited 2018 Jan 22];118:1014–22. Available from: http://www.physiology.org/doi/10.1152/japplphysiol.00441.2014

[42] Sayer AA, Dennison EM, Syddall HE, Gilbody HJ, Phillips DIW, Cooper C. Type 2 diabetes, muscle strength, and impaired physical function: The tip of the iceberg? Diabetes Care. 2005;28:2541–2.

[43] Fernando M, Crowther R, Lazzarini P, Sangla K, Cunningham M, Buttner P, et al. Biomechanical characteristics of peripheral diabetic neuropathy : A systematic review and meta-analysis of findings from the gait cycle , muscle activity and dynamic barefoot plantar pressure. Clin Biomech .2013;28:831–45. Available from: http://dx.doi.org/10.1016/j.clinbiomech.2013.08.004

[44] Ferreira JP, Sartor CD, Leal ÂMO, Sacco ICN, Sato TO, Ribeiro IL, et al. The effect of peripheral neuropathy on lower limb muscle strength in diabetic individuals. Clin Biomech .2017;43:67–73. Available from: http://linkinghub.elsevier.com/retrieve/pii/S0268003317300487

[45] Sacco ICN, Sartor CD. From treatment to preventive actions: improving function in patients with diabetic polyneuropathy. Diabetes Metab Res Rev .2016;32:13–23. Available from: http://libweb.anglia.ac.uk/

[46] 46. Van Schie CHM, Vermigli C, Carrington A, Boulton A. Muscle Weakness and Foot Deformities in Diabetes. Diabetes Care. 2004;27:1668–73.

[47] MacGilchrist C, Paul L, Ellis BM, Howe TE, Kennon B, Godwin J. Lower-limb risk factors for falls in people with diabetes mellitus. Diabet Med. 2010;27:162–8.

[48] Henderson AD, Johnson AW, Ridge ST, Egbert JS, Curtis KP, Berry LJ, et al. Diabetic Gait Is Not Just Slow Gait : Gait Compensations in Diabetic Neuropathy. J Diabetes Res. 2019;2019:1–9.

[49] Labovitz JM, Day D. The Biomechanics of Diabetes Mellitus and Limb Preservation. Clin Podiatr Med Surg. 2019;37:151–69.

[50] Allen MD, Doherty TJ, Rice CL, Kimpinski K. Physiology in Medicine: neuromuscular consequences of diabetic neuropathy. J Appl Physiol. 2016;121:1–6.